HHS Public Access

Author manuscript

Arthritis Rheumatol. Author manuscript; available in PMC 2024 March 01.

Published in final edited form as:

Arthritis Rheumatol. 2023 March ; 75(3): 438–448. doi:10.1002/art.42344.

Increased Expression of LMCD1 in Scleroderma-Associated Interstitial Lung Disease is Critical for Profibrotic Characteristics of Lung Myofibroblasts

Galina S. Bogatkevich, MD, PhD,

Ilia Atanelishvili, MS,

Andrew M. Bogatkevich,

Richard M. Silver, MD

Division of Rheumatology and Immunology, Department of Medicine, Medical University of South Carolina, Charleston, South Carolina, USA

Abstract

Objective: Interstitial lung disease (ILD) is a serious complication and leading cause of mortality in patients with systemic sclerosis (SSc). In the current study we explored the role of LMCD1 (LIM and cysteine-rich domains-1) as a novel factor in the pathogenesis of SSc-ILD.

Material and Methods: Expression and effects of LMCD1 were studied lung tissue and fibroblasts from SSc-ILD patients and control subjects as well as in lung from animal models.

Results: LMCD1 is consistently elevated in lung tissue and in fibroblasts isolated from SSc-ILD patients as compared to controls. Additionally, LMCD1 is highly expressed in the lung in two different animal models of ILD: fibroblast specific protein (FSP)-driven constitutively active TGFβ receptor 1 (FSP-TβR1CA) transgenic and bleomycin-induced mouse models. In lung fibroblasts from SSc-ILD patients LMCD1 is an essential factor for TGFβ-induced generation of collagen type I, fibronectin, and smooth muscle alpha-actin (SMA). Depletion of LMCD1 by siRNA reduces the expression of ECM proteins and lowers transcriptional activity and expression of SMA, as well as decreases proliferation and contractile activity of SSc-ILD lung fibroblasts. In dense fibrotic areas of SSc-ILD lung LMCD1 co-localizes with SMA. In cultured scleroderma lung fibroblasts LMCD1 co-localizes and interacts with serum response factor (SRF) which mediates LMCD1-induced contractile activity of lung fibroblasts.

Conclusion: Our study identifies LMCD1 as a profibrotic molecule contributing to the activation of myofibroblasts and the persistent fibroproliferation observed in SSc-ILD. Thus, LMCD1 may be a potential novel therapeutic target for patients with SSc-ILD.

Keywords

scleroderma; interstitial lung disease; LMCD1; thrombin; TGFβ; fibroblast

Address correspondence and reprint request to Galina S. Bogatkevich, MD, PhD, 96 Jonathan Lucas Street, Suite 816, Medical University of South Carolina, Charleston, SC 29425, Tel.: (843) 792-7631, Fax: (843) 792-7121, bogatkev@musc.edu.

Author Contributions: IA and AMB performed experiments, analyzed data, and reviewed/ edited the draft manuscript. RMS and GSB planned studies, analyzed data, and drafted the manuscript.

Introduction

SSc-ILD is a frequent complication and a leading cause of morbidity and mortality in patients with scleroderma (systemic sclerosis, SSc) (1 – 3). The pathophysiology of SSc-ILD is characterized by differentiation of fibroblasts to activated myofibroblasts with enhanced synthesis and secretion of ECM molecules (4 – 6). The mechanisms leading to lung fibroblast activation with excessive deposition of collagen and other ECM proteins remain poorly understood. A variety of inflammatory and fibrogenic mediators, such as transforming growth factor β (TGFβ), thrombin, platelet-derived growth factor (PDGF), interleukins, and many others have been reported to be involved in the pathogenesis of SSc-ILD (7 – 11). The diversity of the potential mediators suggests multiple pathogenic mechanisms of SSc-ILD and requires complex analysis of the changes that occur in each patient during the course of development of lung disease.

Several groups of investigators have demonstrated a correlation between fibrosis and SMA-expressing myofibroblasts in a number of different tissues (12 – 14). It is generally accepted that lung fibroblasts may differentiate to a myofibroblast phenotype under the influence of local growth factors and cytokines, such as TGF-β and thrombin (7, 9). The transcriptional mechanisms mediating transformation of quiescent fibroblast to myofibroblast, however, have not been fully elucidated.

Proteins that contain LIM domains play a key role in diverse cellular functions, such as signal transduction, cytoskeleton remodeling, cell adhesion and regulation of gene transcription (15). The name of the LIM domain is derived from first letters of three proteins, Lin11, Isl-1, and Mec-3, discovered to contain such motifs. LIM domains represent double-zinc, finger-like structures that mediate protein-protein interactions within distinct subcellular locations and facilitate assembly of multimeric protein complexes (16). Several of the LIM domain-containing proteins have been shown to regulate gene expression by interacting with a variety of general and cell type-specific transcription factors including serum response factor (SRF), which is known to bind to the serum response element (SRE) CArG box (CC(A/T)6GG) found in SMA (17 – 19).

While many of the LIM proteins have been characterized in detail, the cellular functions of LMCD1 are poorly understood. LMCD1 is known to mediate thrombin-induced proliferation and migration of human aortic smooth muscle cells and plays a critical role in the development of cardiac hypertrophy via nuclear factor of activated T cells signaling pathway (20 – 22). Overexpression of LMCD1 has been associated with TGFβ-induced epithelial to mesenchymal transition (23), human hepatocellular carcinoma (24), prostate cancer (25), and alopecia (26). A recently published study demonstrated that LMCD1 regulates tubulointerstitial fibrosis in a mouse model by blocking the activation of the ERK pathway (27). The current study was undertaken to define the role of LMCD1 in fibrosing lung diseases, specifically in SSc-ILD.

Materials and Methods

Animal Models of Lung Fibrosis

All experimental procedures were performed according to guidelines of the Institutional Animal Care and Use Committee (IACUC) at the Medical University of South Carolina (MUSC). The FSP-TβR1CA mouse was established in our laboratory as detailed in the Online Data Supplement. A total of 12 FSP-TβR1CA mice and 12 littermate controls (8 and 12 week old females) were used in this study. Mice with bleomycin-induced ILD were generated as previously described (28, 29). Briefly, lung injury was induced by intratracheal instillation of bleomycin (2U/kg in 50 μl of saline) to the C57BL/6 8-week old mice (n = 6, 3 males and 3 females) obtained from Jackson Laboratories (Bar Harbor, ME). The control mice (n = 6, 3 males and 3 females) received the same volume of saline. Animals were sacrificed on day 21 by isoflurane overdose; lungs were harvested and processed for tissue staining using anti-LMCD1 antibody as described below.

Mouse Lung Fixation and Histological Examinations

Sacrificed mice were subjected to midline thoracotomy. The trachea was cannulated, and the lungs were fixed by instillation of buffered formalin (2%) for 24 hours followed by perfusion with 70% ethanol for another 24 hours before routine processing and paraffin embedding. Multiple sections from each lung were stained with hematoxylin and eosin (H&E) or with trichrome staining for collagen and other extracellular matrix proteins. For the area analysis of fibrotic changes, a quantitative fibrotic scale (Ashcroft scale) was used (30). The severity of fibrotic changes in each lung section was given as the mean score from the observed microscopic fields. Ten fields within each lung section were observed at magnification of x20, and each field was assessed individually for severity and scored from 0 (normal) to 8 (total fibrosis). To avoid bias all histological specimens were evaluated in a blinded fashion. Each specimen was scored independently by two observers, and the mean of individual scores was presented as the fibrosis score. Immunohistochemistry was performed using anti-LMCD1 antibody from Novus Biologicals (Centennial, CO) followed by horseradish peroxidase-conjugated anti-rabbit IgG (Jackson Immunoresearch, W. Grove, PA). Color development was based on metal-enhanced 3,3’-diaminobenzidine (DAB) substrate from Pearce (Rockford, IL). Tissue sections were counterstained for 30 sec by hematoxylin, a nucleus-sensitive dye from Poly Scientific (Bay Shore, NY), mounted using Cytoseal from Stephan Scientific (Kalamazoo, MI) and viewed under a Zeiss microscope (Axiovert 35) using a bright-field mode. The microscope images were obtained digitally (Spot RT Color Digital Camera, Diagnostics Instruments, Sterling Heights, MI) and quantified in a .tiff file format using ImageJ Fiji software as detailed by Crowe and Yue (31). Total cells were identified based on their nuclear staining with hematoxylin. The cells positive for LMCD1 were counted as DAB values over the threshold after background subtracting.

Lung Hydroxyproline Assay

Mouse lung was hydrolyzed in hydrochloric acid and subjected to hydroxyproline determination by Ehrlich reaction as previously described (28). Absorbance was measured at 550 nm, and hydroxyproline content was determined from a standard curve.

Human Lung Tissue Processing and Examinations, Cell Culturing and Transfecting

Lung tissues were collected postmortem from five SSc-ILD patients who fulfilled the 2013 ACR/EULAR classification criteria for SSc (32) and had evidence of lung involvement, and from four age-, race-, and sex-matched control subjects. The diagnosis of SSc-ILD was confirmed by histological examination of postmortem lung tissue. Lung tissues were washed with PBS, fixed in 4% paraformaldehyde, and embedded in paraffin blocks. Seven μm paraffin sections were collected on slides, deparaffinized in histo-clear, and rehydrated through a degrading series of ethanol before staining. Antigen retrieval was performed by Antigen Unmasking solution (Vector Laboratories) and permeabilized for 10 minutes in 0.1% Triton X-100. Nonspecific binding sites were blocked for 40 minutes in Background Buster (Innova Biosciences). The slides were immunostained with anti-LMCD1 antibody from Novus Biologicals (Centennial, CO) and evaluated as described above (mouse histological evaluation). For immunofluorescent staining, the slides were co-stained with anti-LMCD1 and anti-α-Smooth Muscle Actin (SMA) antibodies (Sigma-Aldrich, St. Louis, MO) followed by rabbit Alexa Fluor 555- and CY5 647-conjugated secondary antibodies (Life Technology, Carlsbad, CA). After labeling, slides were mounted with ProLong Gold antifade reagent containing nuclear stain 4′,6-diamidino-2-phenylindole (DAPI), visualized under Zeiss Axio Imager M2 microscope system, and quantified by Adobe Photoshop CS3 software using the Count Tool. Cells stained positively for LMCD1 and SMA were counted directly on the screen by placing markers on the image and counting at least 6 none-overlapping high-power fields at x400 magnification per sample.

Lung fibroblasts were isolated as previously described (33, 34) and used between third and sixth passages in all experiments. LMCD1 siRNA (150pmol per 100-mm dish, 75pmol/well for 6-well plates, and 15pmol/well for 24-well plates) from Santa Cruz Biotechnology (Santa Cruz, CA) was transfected into cells as previously described (35). Scrambled siRNA containing a sequence that does not lead to the specific degradation of any known cellular mRNA was used as a control. Transfection efficiency was routinely tested 48 hours after transfection by immunoblotting with anti-LMCD1 antibody from Novus Biologicals (Centennial, CO).

Immunoblotting and Immunoprecipitation Experiments

Cells were collected and analyzed by immunoblotting as previously described (36). Anti-α-SMA and anti-β-actin antibodies were obtained from Sigma-Aldrich (St. Louis, MO); anti-type I collagen antibody was purchased from SouthernBiotech (Birmingham, AL); anti-fibronectin antibody was obtained from Santa Cruz Biotechnology (Santa Cruz, CA) and anti-LMCD1 antibody was purchased from Novus Biologicals (Centennial, CO). For immunoprecipitation assay, scleroderma lung fibroblasts were grown to confluence on 100mm plates, kept in serum-free DMEM 4 hours, incubated with TGFβ for 24 hours, washed with ice cold PBS, collected with 1ml of ice-cold RIPA buffer, and cleared by microcentrifugation at 4°C. Next, 2μg of anti-SRF antibody (Sigma) was added, and the samples were rotated for 90min at 4°C. Immune complexes were isolated on protein G-sepharose beads (Amersham Pharmacia Biotech, Piscataway, NJ), washed with RIPA buffer, resolved by gel electrophoresis, and immunoblotted with anti-LMCD1 antibody.

RNA isolation and RT-PCR analysis

Cells were cultured in Dulbecco's modified Eagle's medium (DMEM) with or without profibrotic stimuli, such as thrombin or TGFβ in serum-free medium for 24 hours and subjected to total RNA extraction with the RNA Isolation Kit from QIAGEN (Valencia, CA) according to manufacturer's recommendations. RNA purity and amount isolated was determined by spectrophotometric analysis. Reverse transcription was performed with the SuperScript II First-Strand Synthesis Kit from Invitrogen (Carlsbad, CA) and RT-PCR was performed with SYBR Green PCR Master Mix Kit from Bio-Rad (Hercules, CA). PCR primers, synthesized by Eurofins Genomics (Louisville, KY) were as follows: LMCD1 forward AAATTGGCCGCTTGCTGATG, LMCD1 reverse CCCACTCGTAGGTGATGGTG; collagen type I forward CCAGAAGAACTGGTACATCA GCA, collagen type I reverse CGCCATACTCGAACTGGAAT; fibronectin forward CTGACAGCTCATCCGTGGTT, fibronectin reverse CTGAGCTGGTCTGCTTGTCA; SMA forward CCGACCGAATGCAGA AGGA, SMA reverse ACAGAGTATTTGCGCTCCGAA; Glyceraldehyde-3-phosphate dehydrogenase (GAPDH) forward GGTCTCCTCTGACTTCA ACA, GAPDH reverse AGCCAAATTCGTTGTCATAC. RT-PCR was performed on a Bio-Rad MyIQ single color Real-Time PCR detection system under the following conditions: 95°C for 3 min, followed by 35 cycles at 95°C for 30 sec and 60°C for 1 min. Relative differential expression of genes was calculated using the method described by Pfaffl (37) with GAPDH serving as a housekeeping gene. Product size of the gene-specific transcripts was routinely confirmed by agarose gel. Immunoblotting was routinely used to confirm inhibition of LMCD1 expression by siRNA: anti-LMCD1 antibody was purchased from Novus Biologicals (Centennial, CO) and anti-β-actin antibody (as a loading control) was obtained from Sigma-Aldrich (St. Louis, MO).

Quick Cell Proliferation Assay and Cell Counting

Scleroderma lung fibroblasts transfected with LMCD1 or scrambled siRNA were cultured in the absence or presence of thrombin and subjected to the Proliferation Assay and cell counts as described (8).

Luciferase Assay

Cells were cultured in 24-well plates and transfected with SMA promoter luciferase reporter construct (generously provided by Dr. Gerard Elberg, University of Oklahoma Health Sciences Center) using Effectene Transfection Reagent (Qiagen). To investigate effects of LMCD1, cells were co-transfected with LMCD1 siRNA or control siRNA. In all experiments, green fluorescent protein (GFP) plasmid was co-transfected in order to standardize for transfection efficiency. The cells were incubated with TGFβ for 24h and lysed in Passive Lysis Buffer according to the Promega luciferase assay system protocol. The luciferase activity of the cell lysates was measured with luciferase substrate using a luminometer as previously described (38).

Collagen Gel Contraction Assays

Collagen lattices were prepared with type I collagen from rat tail tendons as previously described (7). Lung fibroblasts transfected with LMCD1 siRNA or scrambled siRNA were suspended in collagen, aliquoted into 24 well plates, and cultured for 24 hours. In some experiments cells were transfected with either LMCD1-pCMV6 or SRF-pCMV6 using Effectene Transfection Reagent (Qiagen) and cultured with or without SRF inhibitor CCG-1423 (Selleck Chemicals, Houston, TX). To initiate collagen gel contraction, polymerized gels were gently released from the underlying culture dish and continued to culture for another 24 hours in the presence or absence of TGFβ. Measurement of the diameter of each gel was recorded as the average values of the major and minor axes as previously described (7, 33). Calculation of gel contraction was presented as difference between diameters of wells and contracted gels.

Immunofluorescent studies in lung fibroblasts

SSc-ILD fibroblasts were cultured to sub-confluence on four-chamber slides, serum starved overnight, stimulated with or without TGFβ for 24 hours, fixed with 4% formaldehyde, and blocked with PBS containing 5% BSA, 0.1% Triton, and 0.0004% sodium azide. Cells were incubated overnight with anti-LMCD1 and anti-SRF antibodies (Sigma-Aldrich, St. Louis, MO) followed by rabbit Alexa Fluor 555- and CY5 647-conjugated secondary antibody (Life Technology, Carlsbad, CA). Next, slides were washed with PBS, mounted with ProLong Gold antifade reagent and visualized under Olympus FV10i laser scanning confocal or Zeiss Axio Imager M2 microscope system.

Cell Fractionation Assay

Lung fibroblasts were cultured in 100 mm plates, serum starved overnight, and stimulated with or without TGFβ for 24 hours. Nuclear and cytoplasmic proteins were isolated using Abcam's Cell Fractionation Kit following the detailed instructions provided by the manufacturer. Tubulin antibody from Sigma and Histone-H3 antibody from Cell Signaling were used to screen purity of cytoplasm and nuclear fraction.

Statistical Analysis

Statistical analyses were performed using analysis of variance models followed by *post hoc* testing or nonparametric test as appropriate. The results were considered significant if $p<0.05$.

Results

Expression of LMCD1 is increased in two animal models of lung fibrosis

We examined the expression of LMCD1 in two different animal models of pulmonary fibrosis. The FSP-TβR1CA transgenic mouse is characterized by constitutive activation of the TGFβ receptor 1 (39) in fibroblasts and other cells expressing FSP. Recombination of TβR1CA and FSP-Cre alleles at the genomic DNA level was routinely confirmed in 3-week old pups by genotyping; see Online Data Supplement and Figure S1 for details. The FSP-TβR1CA mice appeared phenotypically normal but spontaneously developed chronic

fibrosis in the lung beginning at week 8. Importantly, lung fibrosis in the FSP-TβR1CA mice appears first in the subpleural portion of the lung showing diffuse involvement of the alveolar walls with thickening and loss of alveoli (Figure 1A) closely resembling SSc-ILD. The overall level of fibrotic changes was quantitatively assessed in the 8- and 12-week old mice using the Ashcroft scoring system. The Ashcroft score was 3.02-fold higher in the 8-week old FSP-TβR1CA mice and 4.44-fold higher in the 12-week old FSP-TβR1CA mice when compared to the control littermates (Figure 1B).

Progressive increase of collagen in the lungs of FSP-TβR1CA mice was demonstrated by hydroxyproline assays (Figures 1C). Immunostaining showed that LMCD1 was substantially elevated in lung tissue from FSP-TβR1CA mice as compared to control littermates (Figure 2A and 2B). Quantification of LMCD1-stained lung tissue from 12-week old FSP-TβR1CA mice demonstrated significant increase of LMCD1-positive cells, equal to 69.34 ± 4.76% of total cells as compared to 9.55 ± 1.82% of cells in lung tissue from the control littermates ($p < 0.0001$), Figure 2C).

Bleomycin-induced mouse model of pulmonary fibrosis is described in detail in our previous publications (28, 29). Immunohistochemistry for LMCD1 in serial sections of lung tissue from mice receiving bleomycin showed that LMCD1 was strongly up-regulated in fibrotic lung tissue reaching 65.22 ± 8.25% of total cells from bleomycin-treated mice, while only 3.28 ± 1.22% of cells from saline-treated mice expressed LMCD1 (Figure 2D – F).

Expression of LMCD1 in SSc-ILD

To establish the presence and localization of LMCD1 within lung tissue of SSc-ILD patients, we employed immunohistochemistry to stain for LMCD1 in sequential sections of lung tissue from patients with end-stage SSc-ILD and from age-, race-, and sex-matched healthy control subjects. We observed that LMCD1 expression is dramatically increased in lung tissue from SSc-ILD patients, mainly in the lung parenchyma where it is seen in association with inflammatory and fibroproliferative foci (Figure 2G and 2H). Quantitative analysis demonstrated that expression of LMCD1 in lung tissue from patients with SSc-ILD is significantly higher ($p < 0.001$) compared with lung tissue from controls. Only 10.37±4.51 % of total cells in control lung tissue expressed LMCD1 as compared to 64.79±12.10 % of LMCD1-positive cells in SSc-ILD lung tissue (Figure 2I).

To determine whether LMCD1 is expressed in myofibroblasts, we performed double immunofluorescence staining of SSc-ILD lung sections for LMCD1 and SMA. We observed that in dense fibrotic areas of SSc-ILD lung 69.18±14.10 % of total cells express LMCD1 and 66.56±14.18 % of total cells express SMA; importantly, nearly all SMA-positive cells expressed LMCD1 (Figure 3A–E).

To examine expression of LMCD1 in isolated scleroderma lung fibroblasts, we used three SSc-ILD cell lines and three normal lung fibroblast cells lines from matched controls. We found that mRNA levels of LMCD1 in SSc-ILD fibroblasts significantly ($p < 0.01$) exceeds mRNA levels of LMCD1 in normal lung fibroblasts (Figure 3F). We incubated lung fibroblasts with either thrombin or TGFβ for 24 hours and observed that thrombin augments expression of LMCD1 mRNA 3.11-fold in normal and 1.77-fold in scleroderma

lung fibroblasts. Similar to thrombin, TGFβ increased LMCD1 mRNA 2.93-fold in normal and 1.72-fold in scleroderma lung fibroblasts (Figure 3F).

Effects of LMCD1 depletion on extracellular matrix proteins in SSc lung fibroblasts

To establish whether LMCD1 is involved in generation of ECM in SSc lung fibroblasts, we knocked down LMCD1 expression by siRNA and used TGFβ to stimulate production of ECM proteins in SSc lung fibroblasts. Immunoblotting experiments demonstrated that transfection of cells with LMCD1 siRNA resulted in a significant reduction of LMCD1 protein in SSc lung fibroblasts as well as decreasing basal and TGFβ-induced levels of fibronectin, collagen type I, and SMA in SSc lung fibroblasts (Figure 4A).

Effects of LMCD1 depletion on TGFβ-induced fibronectin and collagen type I mRNA was studied by RT-PCR. Expression of fibronectin mRNA and collagen type I mRNA in SSc lung fibroblasts stimulated with TGFβ in a concentration 2.5 ng/ml for 24h increased 5.3-fold and 19.8-fold respectively as compared to unstimulated cells. Depletion of LMCD1 by siRNA significantly reduced levels of TGFβ-induced fibronectin mRNA (1.86-fold, $p < 0.01$) and collagen type I mRNA (1.94-fold, $p < 0.01$) (Figure 4B and C).

LMCD1 mediates expression of SMA and contractile activity of SSc-ILD lung fibroblasts

Regulation of TGFβ-induced SMA expression by LMCD1 was studied by RT-PCR as well. We found that depletion of LMCD1 by siRNA significantly reduces basal (2.29-fold, $p < 0.001$) and TGFβ-induced SMA expression (1.97-fold, $p < 0.01$) (Figure 4D).

To determine whether LMCD1 mediates transcription of SMA in SSc-ILD lung fibroblasts, we transfected cells with LMCD1 siRNA or scrambled siRNA as a control and performed a luciferase reporter assay. We observed that TGFβ increases the transcriptional activity of the SMA promoter 8.78-fold in scleroderma lung fibroblasts transfected with control siRNA. When cells were transfected with LMCD1 siRNA, activity of the SMA promoter induced by TGFβ was reduced by nearly 3.88-fold (Figure 4E).

To investigate whether depletion of LMCD1 affects contractile activity of SSc lung fibroblasts, we performed collagen gel contraction assays. We observed that SSc lung fibroblasts transfected with scrambled siRNA contracted gels to 9.32±1.57 mm, whereas cells transfected with LMCD1 siRNA contracted gels significantly less (to 4.02±0.94 mm, $p<0.001$) (Figure 4F). TGFβ further enhanced contractile activity of SSc lung fibroblasts increasing collagen gel contraction to 11.37±1.4 mm in cells transfected with scrambled siRNA; however, contractile activity of TGFβ-stimulated SSc lung fibroblasts significantly decreased ($p<0.001$) to 4.78±1.34 mm in cells transfected with LMCD1 siRNA (Figure 4F).

LMCD1 mediates proliferation of SSc-ILD lung fibroblasts

We previously reported that thrombin is one of the strongest inducers of lung fibroblast proliferation in SSc-ILD (7, 10). To study effects of LMCD1 depletion on thrombin-induced lung fibroblast proliferation, we employed a quick cell proliferation assay. Basal levels of viable scleroderma lung fibroblasts transfected with scrambled siRNA were 0.43±0.04 optical density (OD) units. Basal levels of cells transfected with LMCD1 siRNA were

significantly lower (0.21±0.04 OD units, $p < 0.001$). Thrombin increased the proliferative capacity of cells transfected with scrambled siRNA, whereas thrombin-induced proliferation was significantly reduced to 0.41±0.08 OD in cells transfected with LMCD1 siRNA ($p < 0.001$) (Figure 5A), suggesting that LMCD1 mediates thrombin-induced proliferation of SSc-ILD fibroblasts.

To measure time-dependent effects of LMCD1 depletion on thrombin-induced proliferation of SSc lung fibroblasts, we stimulated siRNA-transfected cells with thrombin for 24h, 48h, 72h, and 96h. The proliferation rate of cells transfected with control siRNA and stimulated with thrombin was increased 2.13-fold within 24h and further increased 3.23-fold within 96h. Depletion of LMCD1 significantly ($p<0.001$) inhibited thrombin-induced proliferation of SSc lung fibroblasts at all time points measured. The proliferation rate of cells transfected with LMCD1 siRNA and stimulated with thrombin was reduced 2.1-fold within 24h, 1.94-fold within 48h, 2.07-fold within 72h, and 2.1-fold within 96h as compared to cells transfected with control siRNA (Figure 5B).

Localization pattern of LMCD1 in SSc-ILD lung fibroblasts

We observed that LMCD1 has nuclear, cytoplasmic, and cytoskeletal localizations in SSc-ILD fibroblasts (Online Data Supplement, Figure S3). To elucidate whether profibrotic stimuli affect the localization pattern of LMCD1 in lung fibroblasts, we cultured cells in the presence or absence of TGFβ for 24 hours followed by cell fractionation into cytoplasmic and nuclear fractions. Unexpectedly, we found that LMCD1 was predominantly localized in the cytoplasm with and without TGFβ stimulation; TGFβ-induced expression of LMCD1 in cytoplasmic and nuclear fractions was proportional to the TGFβ-induced expression of LMCD1 in total cell lysate (Figure 5C).

We found that despite predominant localization in the cytoplasm, LMCD1 immunoprecipitates with SRF, which is known to localize mostly in the nuclei of proliferating cells (40) suggesting direct interaction between these proteins. We observed that the immunoprecipitation was enhanced after SSc-ILD fibroblasts were cultured with TGFβ (Figure 5D). To further confirm interaction between LMCD1 and SRF, we cultured SSc-ILD fibroblasts on glass slides with and without TGFβ and performed immunofluorescent staining of the cells. Immunofluorescent studies confirmed that in SSc lung fibroblasts, predominant localization of LMCD1 is the cytoplasm either with or without TGFβ stimulation. However, after stimulation with TGFβ, cells generate more LMCD1, and co-localization of LMCD1 with SRF is increased in nuclear, perinuclear, and cytoplasmic regions (Figure 6 A–J).

SRF is essential for LMCD1-mediated contractile activity of lung fibroblasts.

Data presented in Figure 4 demonstrate that depletion of LMCD1 with siRNA reduces contractile activity of SSc lung fibroblasts. To investigate whether SRF affects LMCD1-modulated contractile activity of SSc lung fibroblasts, we co-transfected cells with LMCD1 siRNA and recombinant SFR. Contractile activity of cells co-transfected with LMCD1 siRNA and empty pCMV6 vector was reduced from 9.47±2.06 mm to 4.25±0.93 mm. Contractile activity of cells co-transfected with LMCD1 siRNA and SRF in pCMV6,

however, was 8.97±1.76, similar to SSc-ILD control lung fibroblasts (Figure 6K). These data demonstrate that overexpression of SRF restores the contractile activity of SSc lung fibroblasts reduced by LMCD1 siRNA. To verify the importance of SRF in LMCD1-induced contractile activity of lung fibroblasts, normal lung fibroblasts transfected with recombinant LMCD1 were cultured in collagen gels in the presence of SRF pathway inhibitor CCG-1423. Control cells transfected with empty vector were characterized by low contractile activity (4.38±1.1 mm). Recombinant LMCD1 significantly enhanced contractile activity of lung fibroblasts by increasing contraction of collagen gels to 8.6±1.562 mm ($p < 0.01$) (Figure 6L). SRF inhibition completely blocked LMCD1-induced contractile activity, decreasing contraction of collagen gels to 4.15±1.09 mm but had no effect on cells transfected with empty vector suggesting that SRF mediates LMCD1-induced contractile activity in lung fibroblasts.

Discussion

Despite its clinical and public health significance, the pathophysiology of SSc-ILD or any other ILD remains insufficiently understood. The current study identifies LMCD1 as a novel protein involved in major profibrotic signaling in scleroderma lung myofibroblasts.

LMCD1 is a transcriptional cofactor containing a cysteine-rich domain in the N-terminal region and two double zinc-finger LIM domains in the C-terminal region (20 – 22). The presence of LIM domains suggests involvement of LMCD1 in protein-protein interactions as LIM domains are known to mediate communications between transcription factors, cytoskeletal proteins, and signaling proteins (15, 16).

LMCD1 is expressed in many tissues with highest abundance in skeletal muscle (41). Here we demonstrate that LMCD1 protein is present in normal lung tissue at very low levels, whereas it is highly upregulated in SSc-ILD lung tissue. To demonstrate that LMCD1 is upregulated in mouse fibrotic lung tissues, we studied expression of LMCD1 in two different animal models of ILD: the FSP-TβR1CA transgenic mouse model and the bleomycin-induced mouse model of pulmonary fibrosis. Animal models of ILD have been useful in revealing the pathobiology of SSc-ILD and identifying potential new therapeutic targets (42). We observed that expression patterns of LMCD1 in mouse lung tissue is very similar to its expression in human lung: low expression in control lung tissue and highly upregulated expression in fibrotic lung tissue, which suggests that elevated LMCD1 protein expression follows from a number of different fibrotic triggers.

Among various cell lines, lung fibroblasts are the most prominent cells that contribute to the pathogenesis of SSc-ILD (4). We observed that SSc-ILD fibroblasts contain higher amount of LMCD1 as compared to normal lung fibroblasts and that well-known profibrotic factors such as thrombin and TGFβ further increased expression of LMCD1 in both normal and scleroderma lung fibroblasts.

Lung fibroblasts derived from SSc-ILD patients are characterized by increased proliferative capacity and by high expression of ECM proteins such as collagen type I and fibronectin (7, 8). Thrombin is a major mitogen for mesenchymal cells and one of the strongest identified

proliferative stimulus for fibroblasts (7, 10), whereas TGFβ is a major inducer of ECM genes and proteins in scleroderma fibroblasts (9). Depletion of LMCD1 by siRNA reduced thrombin-stimulated and basal proliferation of SSc-ILD fibroblasts. Depletion of LMCD1 by siRNA also downregulated expression of fibronectin and collagen type I, signifying a role of LMCD1 as an important profibrotic molecule in lung fibroblasts.

During progression of the disease, SSc-ILD fibroblasts differentiate to highly contractile myofibroblasts that synthesize excessive amounts of SMA (7). Here we demonstrate for the first time that LMCD1 is necessary for transcriptional activity and protein expression of SMA, which suggests that LMCD1 might work as a positive transcriptional regulator of myofibroblasts. To examine whether LMCD1 contributes to the increased contractile capacities of scleroderma myofibroblasts, we performed contraction assays of floating collagen gels populated with SSc-ILD fibroblasts. This assay mimics the initial phase of fibrosis reflecting the induction of the myofibroblast phenotype by various growth factors (32, 43). We observed that depletion of LMCD1 in SSc-ILD fibroblasts inhibits basal and TGFβ-induced collagen gel contraction, thus suggesting that LMCD1 may promote the contractile features seen in SSc-ILD.

It is well established that transcription of SMA is mediated by SRF (19, 44). It is also known that SRF interacts with several of the LIM domain-containing proteins in smooth muscle cells and other mesenchymal cells (17 – 19). Expression of SRF in lung mesenchyme was recently shown to be essential for development of pulmonary fibrosis (45). Here we demonstrate that SRF co-localizes and interacts with LMCD1 in scleroderma lung fibroblasts mediating LMCD1-induced contractile activity of lung fibroblasts.

We postulate that LMCD1 is an essential profibrotic mediator in ILD that exerts its fibrogenic effects via interaction with transcription factors. On the other hand, a predominant cytoplasmic localization pattern of LMCD1 suggests that LMCD1 may regulate fibrogenesis by targeting cytoplasmic substrates. Further studies including those using an LMCD1 knockout mouse are necessary to delineate more of LMCD1’s fibrogenic mechanisms.

In conclusion, the results presented here are the first to demonstrate that LMCD1 is highly expressed in fibrotic lung tissue and upregulated by prominent profibrotic factors implicated in the differentiation of fibroblasts to myofibroblasts. As multiple networks of numerous molecules and cells control the complex processes of tissue injury, repair and remodeling in SSc-ILD, LMCD1 might serve as a driver of the underlying transcriptional mechanisms leading to the development of the activated myofibroblasts and producing an overabundance of ECM proteins leading to lung fibrosis. Thus, LMCD1 may be a potential target for much needed novel therapy for SSc-ILD as well as other fibrosing lung diseases.

Supplementary Material

Refer to Web version on PubMed Central for supplementary material.

Acknowledgments

This study was supported in part by a grant from National Scleroderma Foundation and by the SC SmartState Centers. De-identified lung tissues were provided by the MUSC CCCR (NIH/NIAMS P30 AR072582). Imaging core was supported by South Carolina COBRE for Developmentally Based Cardiovascular Diseases (NIH-NIGMS P30 GM103342).

References

1. Furst DE, Fernandes AW, Iorga SR, Greth W, Bancroft T. Epidemiology of systemic sclerosis in a large US managed care population. J Rheumatol 2012;39:784–6. [PubMed: 22382343]
2. Perelas A, Arrossi AV, Highland KB. Pulmonary Manifestations of Systemic Sclerosis and Mixed Connective Tissue Disease. Clin Chest Med 2019;40(3):501–518. [PubMed: 31376887]
3. Ostojic P, Cerinic MM, Silver R, Highland K, Damjanov N. Interstitial lung disease in systemic sclerosis. Lung 2007;185(4):211–20. [PubMed: 17717851]
4. Akter T, Silver RM, Bogatkevich GS. Recent advances in understanding the pathogenesis of scleroderma-interstitial lung disease. Curr Rheumatol Rep 2014;16(4):411. [PubMed: 24523015]
5. Tomasek JJ, Gabbiani G, Hinz B, Chaponnier C, Brown RA. Myofibroblasts and mechano-regulation of connective tissue remodeling. Nat Rev Mol Cell Biol 2002;3(5):349–63 [PubMed: 11988769]
6. Gyftaki-Venieri DA, Abraham DJ, Ponticos M. Insights into myofibroblasts and their activation in scleroderma: opportunities for therapy? Curr Opin Rheumatol 2018;30(6):581–587. [PubMed: 30074511]
7. Bogatkevich GS, Tourkina E, Silver RM and Ludwicka-Bradley A: Thrombin differentiates normal lung fibroblast to a myofibroblast phenotype via proteolytically activated receptor-1 and protein kinase C-dependent pathway. J Biol Chem 2001; 276, 45184–92. [PubMed: 11579091]
8. Atanelishvili I, Akter T, Noguchi A, Vuyiv O, Wollin L, Silver RM, Bogatkevich GS. Antifibrotic efficacy of nintedanib in a cellular model of systemic sclerosis-associated interstitial lung disease. Clin Exp Rheumatol 2019;37 Suppl 119(4):115–124. [PubMed: 31573469]
9. Lafyatis R Transforming growth factor β at the centre of systemic sclerosis. Nat Rev Rheumatol 2014;10:706–719. [PubMed: 25136781]
10. Ohba T, McDonald JK, Silver RM, Strange C, LeRoy EC and Ludwicka A. Scleroderma BAL fluid contains thrombin, a mediator of human lung fibroblast proliferation via induction of the PDGF-alpha receptor. Am J Resp Cell Mol Biol 1994; 10:405–12.
11. Khanna D, Tashkin DP, Denton CP, Renzoni EA, Desai SR, Varga J. Etiology, Risk Factors, and Biomarkers in Systemic Sclerosis with Interstitial Lung Disease. Am J Respir Crit Care Med 2020;201:650–660. [PubMed: 31841044]
12. Scotton CJ, Chambers RC. Molecular targets in pulmonary fibrosis: the myofibroblast in focus. Chest 2007;132:1311–21. [PubMed: 17934117]
13. Gabbiani G The myofibroblast in wound healing and fibrocontractive diseases. J Pathol 2003; 200:500–03. [PubMed: 12845617]
14. Schulz JN, Plomann M, Sengle G, Gullberg D, Krieg T, Eckes B. New developments on skin fibrosis - Essential signals emanating from the extracellular matrix for the control of myofibroblasts. Matrix Biol 2018;68-69:522–532. [PubMed: 29408278]
15. Kadrmas JL, Beckerle MC. The LIM domain: from the cytoskeleton to the nucleus. Nat Rev Mol Cell Biol 2004;5:920–931. [PubMed: 15520811]
16. Bhati M, Lee C, Nancarrow AL, Lee M, Craig VJ, Bach I et al. Implementing the LIM code: the structural basis for cell type-specific assembly of complexes recruited by LIM homeodomain transcription factors. EMBO J 2008; 27, 2018–2029. [PubMed: 18583962]
17. Philippar U, Schratt G, Dieterich C, Muller JM, Galgoczy P, Engel FB et al. The SRF target gene Fhl2 antagonizes RhoA/MAL-dependent activation of SRF. Mol Cell 2004;16:867–880. [PubMed: 15610731]

18. Chang DF, Belaguli NS, Iyer D, Roberts WB, Wu SP, Dong XR et al. Cysteine-rich LIM-only proteins CRP1 and CRP2 are potent smooth muscle differentiation cofactors. Dev Cell 2003;4:107–118. [PubMed: 12530967]
19. Miralles F, Posern G, Zaromytidou AI, Treisman R. Actin dynamics control SRF activity by regulation of its coactivator MAL. Cell 2003;113:329–42. [PubMed: 12732141]
20. Bian ZY, Huang H, Jiang H, Shen DF, Yan L, Zhu LH et al. LIM and cysteine-rich domains 1 regulates cardiac hypertrophy by targeting calcineurin/nuclear factor of activated T cells signaling. Hypertension. 2010;55:257–263. [PubMed: 20026769]
21. Frank D, Frauen R, Hanselmann C, Kuhn C, Will R, Gantenberg J et al. Lmcd1/Dyxin, a novel Z-disc associated LIM protein, mediates cardiac hypertrophy in vitro and in vivo. J Mol Cell Cardiol 2010;49:673–682. [PubMed: 20600098]
22. Janjanam J, Zhang B, Mani AM, Singh NK, Traylor JG Jr, Orr AW, Rao GN. LIM and cysteine-rich domains 1 is required for thrombin-induced smooth muscle cell proliferation and promotes atherogenesis. J Biol Chem 2018;293:3088–3103. [PubMed: 29326163]
23. Du L, Yamamoto S, Burnette BL, Huang D, Gao K, Jamshidi N, Kuo MD. Transcriptome profiling reveals novel gene expression signatures and regulating transcription factors of TGFβ-induced epithelial-to-mesenchymal transition. Cancer Med 2016;5:1962–1972. [PubMed: 27318801]
24. Chang CY, Lin SC, Su WH, Ho CM, Jou YS. Somatic LMCD1 mutations promoted cell migration and tumor metastasis in hepatocellular carcinoma. Oncogene. 2012;31:2640–2652. [PubMed: 21996735]
25. Dmitriev AA, Rosenberg EE, Krasnov GS, Gerashchenko GV, Gordiyuk VV, Pavlova TV et al. Identification of novel epigenetic markers of prostate cancer by notI-microarray analysis. Dis Markers. 2015;2015:241301. [PubMed: 26491211]
26. Muhammad SA, Fatima N, Paracha RZ, Ali A, Chen JY. A systematic simulation-based meta-analytical framework for prediction of physiological biomarkers in alopecia. J Biol Res (Thessalon) 2019;26:2. [PubMed: 30993080]
27. Yu R, Tian M, He P, Chen J, Zhao Z, Zhang Y, Zhang B. Suppression of LMCD1 ameliorates renal fibrosis by blocking the activation of ERK pathway. Biochim Biophys Acta Mol Cell Res. 2022;1869(4):119200. [PubMed: 34968577]
28. Bogatkevich GS, Ludwicka-Bradley A, Nietert PJ, Akter T, van Ryn J, Silver RM. Anti-inflammatory and anti-fibrotic effects of the oral direct thrombin inhibitor dabigatran etexilate in a murine model of interstitial lung disease. Arthritis Rheum 2011;63:1416–25. [PubMed: 21312187]
29. Atanelishvili I, Shirai Y, Akter T, Buckner T, Noguchi A, Silver RM, Bogatkevich GS. M10, a caspase cleavage product of the hepatocyte growth factor receptor, interacts with Smad2 and demonstrates antifibrotic properties in vitro and in vivo. Transl Res 2016;170:99–111. [PubMed: 26772959]
30. Ashcroft T, Simpson JM, Timbrell V. Simple method of estimating severity of pulmonary fibrosis on a numerical scale. J Clin Pathol 1988;41:467–70. [PubMed: 3366935]
31. Crowe AR, Yue W. Semi-quantitative Determination of Protein Expression using Immunohistochemistry Staining and Analysis: An Integrated Protocol. Bio Protoc. 2019; 9(24):e3465. doi: 10.21769/BioProtoc.3465.
32. van den Hoogen F, Khanna D, Fransen J, Johnson SR, Baron M, Tyndall A, Matucci-Cerinic M et al. 2013 classification criteria for systemic sclerosis: an American College of Rheumatology/ European League against Rheumatism collaborative initiative. Arthritis Rheum. 2013;65:2737–47. [PubMed: 24122180]
33. Bogatkevich GS, Ludwicka-Bradley A, and Silver RM. Dabigatran, a direct thrombin inhibitor, demonstrates antifibrotic effects on lung fibroblasts. Arthritis Rheum 2009; 60: 3455–3464, 2009.
34. Atanelishvili I, Shirai Y, Akter T, Noguchi A, Ash KT, Misra S, Ghatak S et al. D1398G Variant of MET Is Associated with Impaired Signaling of Hepatocyte Growth Factor in Alveolar Epithelial Cells and Lung Fibroblasts. PloS one 2016; 11: e0162357. [PubMed: 27584154]
35. Bogatkevich GS, Ludwicka-Bradley A, Singleton CB, Bethard JR, and Silver RM. Proteomic analysis of CTGF-activated lung fibroblasts: identification of IQGAP1 as a key player in lung fibroblast migration. Am J Physiol: Lung Cell Mol Physiol 2008; 295: L603–611. [PubMed: 18676875]

36. Akter T, Atanelishvili I, Shirai Y, Garcia-Martos A, Silver RM, Bogatkevich GS. IQGAP1 Mediates α-Smooth Muscle Actin Expression and Enhances Contractility of Lung Fibroblasts. Rheum (Sunnyvale) 2018;8:242. doi:10.4172/2161-1149.1000242
37. Pfaffl MW: A new mathematical model for relative quantification in real-time RT–PCR. Nucl Acids Res 2001; 29: 2002–7.
38. Atanelishvili I, Liang J, Akter T, Spyropoulos DD, Silver RM and Bogatkevich GS. Thrombin increases lung fibroblast survival while promoting alveolar epithelial cell apoptosis via the ER stress marker CHOP. Am J Respir Cell Mol Biol 2014; 50:893–902. [PubMed: 24279877]
39. Bartholin L, Cyprian FS, Vincent D, Garcia CN, Martel S, Horvat B et al. Generation of mice with conditionally activated transforming growth factor beta signaling through the TbRI/ALK5 receptor. Genesis 2008; 46:724–731. [PubMed: 18821589]
40. Ding W, Gao S, Scott RE. Senescence represses the nuclear localization of the serum response factor and differentiation regulates its nuclear localization with lineage specificity. J Cell Sci. 2001;114:1011–8. [PubMed: 11181183]
41. Bespalova IN, Burmeister M. Identification of a novel LIM domain gene, LMCD1, and chromosomal localization in human and mouse. Genomics 2000;63:69–74. [PubMed: 10662546]
42. B Moore B, Lawson WE, Oury TD, Sisson TH, Raghavendran K, Hogaboam CM. Animal models of fibrotic lung disease. Am J Respir Cell Mol Biol 2013;49:167–79. [PubMed: 23526222]
43. Grinnell F Signal transduction pathways activated during fibroblast contraction of collagen matrices. Curr Top Pathol 1999;93:61–73. [PubMed: 10339899]
44. Fan L, Sebe A, Péterfi Z, Masszi A, Thirone AC, Rotstein OD et al. Cell contact-dependent regulation of epithelial-myofibroblast transition via the rho-rho kinase-phospho-myosin pathway. Mol Biol Cell 2007;18(3):1083–97. [PubMed: 17215519]
45. Bernau K, Leet JP, Bruhn EM, Tubbs AJ, Zhu T, Sandbo N. Expression of serum response factor in the lung mesenchyme is essential for development of pulmonary fibrosis. Am J Physiol Lung Cell Mol Physiol. 2021;321(1):L174–L188. [PubMed: 33978489]

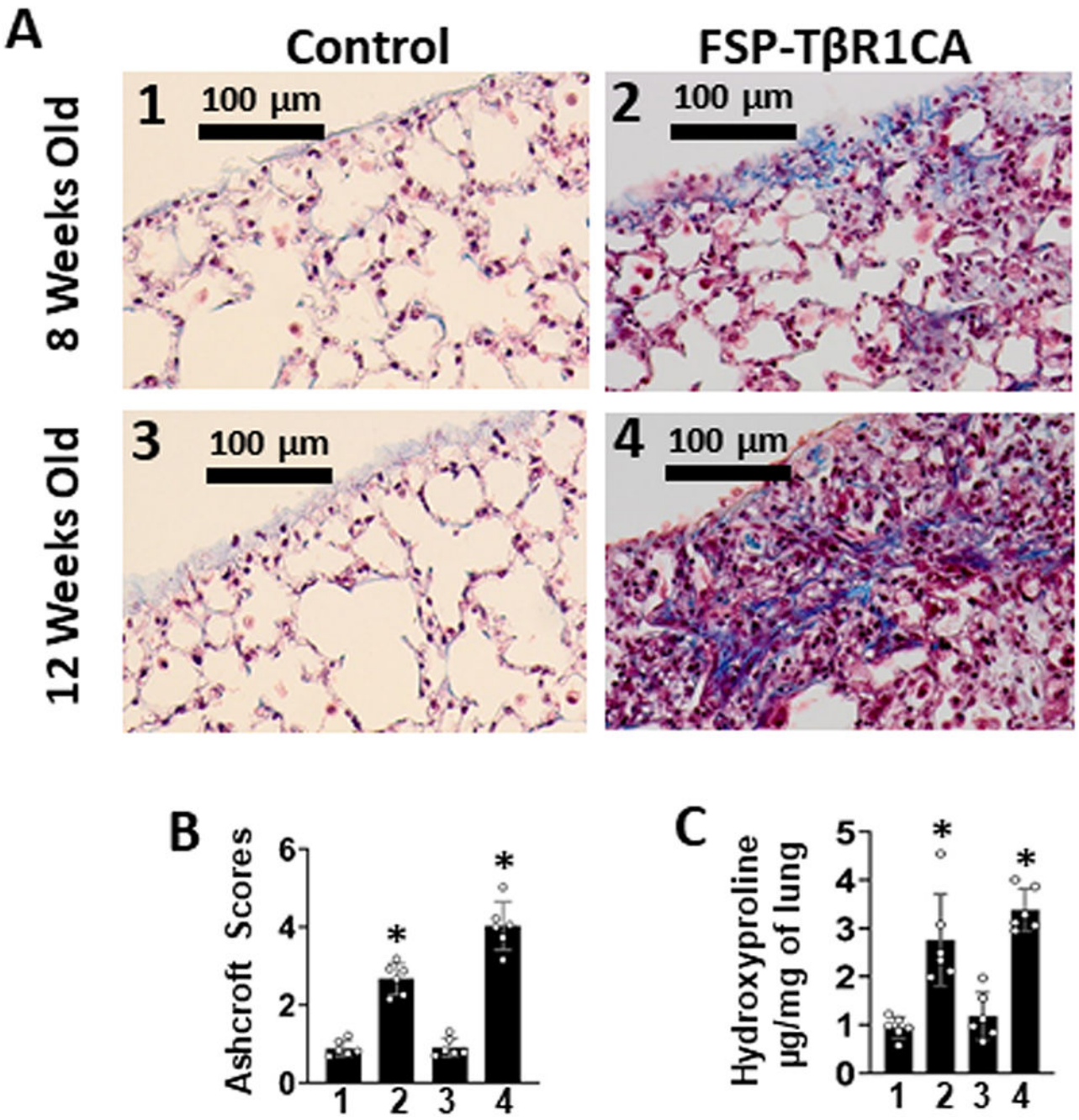

Figure 1. FSP-TβR1CA mice spontaneously develop lung fibrosis.

A, representative histological images of Trichrome-stained lung sections of FSP-TβR1CA mice (images 2 and 4) and littermate control mice (images 1 and 3) sacrificed at 8 weeks (images 1 and 2) and 12 weeks (images 3 and 4). **B**, quantitative evaluation of fibrotic changes (Ashcroft scores). **C**, lung collagen content determined by Hydroxyproline assay. N = 24 (six mice per group). Values are the mean ± SD. *statistically significant differences ($P < 0.05$) between FSP-TβR1CA and littermate control mice.

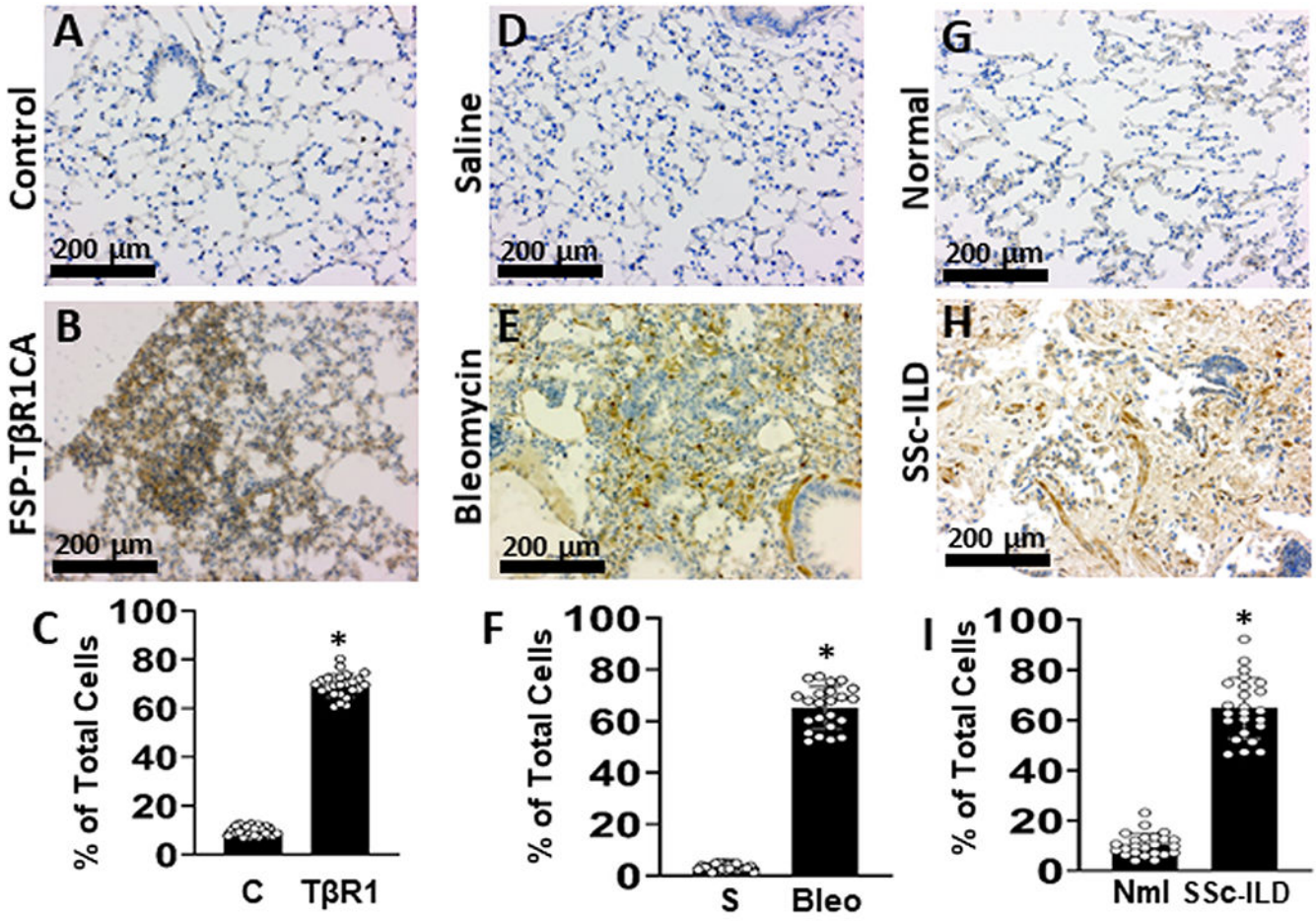

Figure 2. LMCD1 is over-expressed in animal models of pulmonary fibrosis and in lung tissue of SSc-ILD patients.

Sections of normal lung tissue isolated from littermate controls of 12-week-old FSP-TβR1CA mice (**A**), saline-treated C57BL/6 mice (**D**), human normal lung tissue (**G**) and sections of fibrotic lung tissue from 12-week-old FSP-TβR1CA mice (**B**), bleomycin-treated C57BL/6 mice (**E**), and SSc-ILD patients **(H)** were stained with anti-LMCD1 antibody. Representative images of 4 samples per each group are presented. **C, F and I**, quantitative results of image analysis for LMCD1-positive cells. Cells (total and LMCD1-positive) were counted on randomly selected 6 non-overlapping high-power fields per each sample. Values are the mean ± SD. * = $P < 0.0001$.

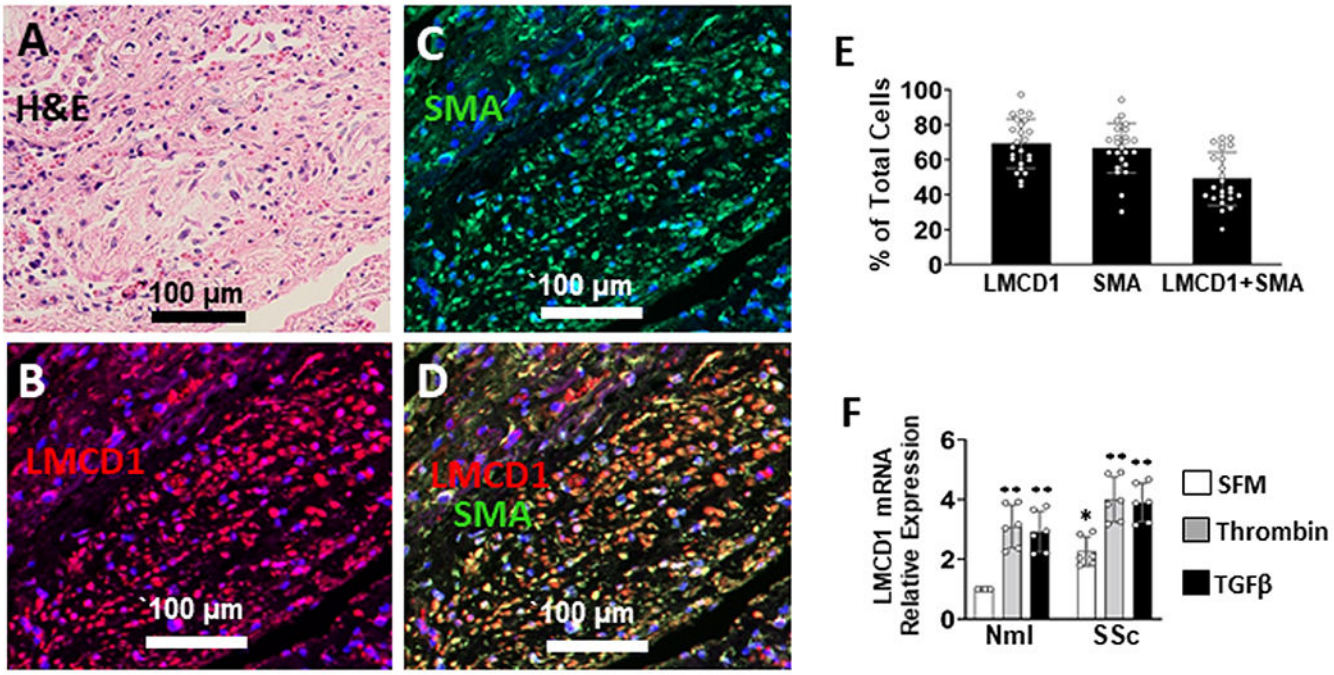

Figure 3. Expression of LMCD1 in lung fibroblasts in areas of dense fibrosis in patients with SSc-ILD.

Representative images of lung sections from 4 SSc-ILD patients stained with H&E (**A**), anti-LMCD1 (**B**), and anti-SMA (**C**) antibodies are presented; nuclei are stained with DAPI. (**D**) Merged immunofluorescent image of LMCD1 with SMA. (**E**) Quantification of LMCD1- and SMA-positive cells. Lung sections from 4 SSc-ILD patients were analyzed at x400 magnification. Data represent means ± SD from randomly selected 6 none-overlapping high-power fields. **F**, expression of LMCD1 mRNA in normal (Nml) and scleroderma (SSc) lung fibroblasts. Cells were cultured in the presence or absence of thrombin or TGFβ for 24 h. Data are presented as means ± SD. The asterisk represents statistically significant differences ($p<0.01$) between SSc and Nml lung fibroblasts. Double asterisks represent statistically significant differences ($p<0.01$) between cells treated with thrombin or TGFβ *vs.* non-treated cells.

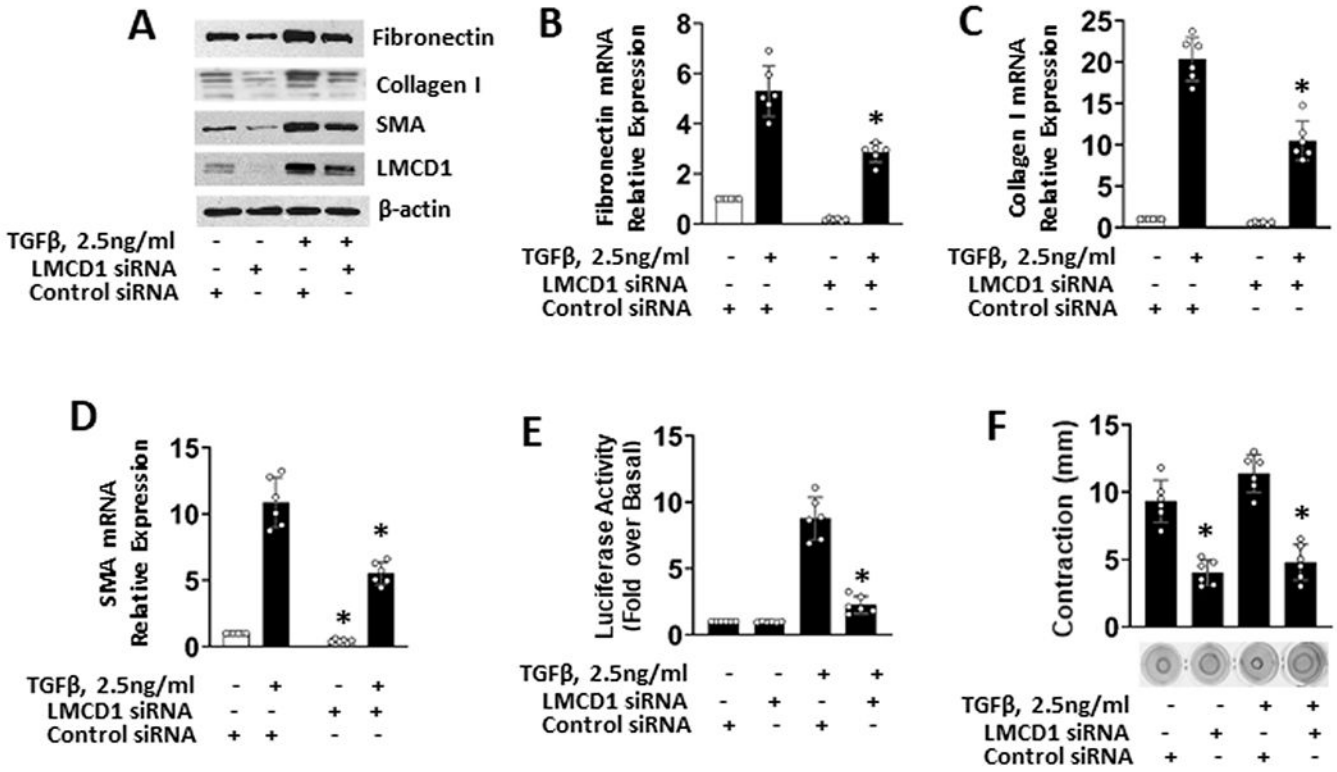

Figure 4. LMCD1 and collagen I, fibronectin, SMA and contractile activity of SSc-ILD lung fibroblasts.

A, cell lysates were analyzed by Western blot with LMCD1 antibody as a transfection efficiency control and anti-β-actin antibody as a loading control. Depletion of LMCD1 by siRNA diminishes mRNA of fibronectin (**B**), collagen type I (**C**), and SMA (**D**) in SSc lung fibroblasts. **E**, LMCD1 siRNA reduces TGFβ-induced transcriptional activity of the SMA promoter. Data are expressed as relative luciferase signal normalized by the green fluorescent protein signal for each individual analysis. **F**, LMCD1 siRNA attenuates contractile activity of SSc lung fibroblasts. The degree of collagen gel contraction was determined as the difference between diameters of well and released gels. All data are presented as mean values ± SD of three independent experiments each performed in duplicate. The *asterisk* represents statistically significant differences ($p<0.001$) between cells transfected with LMCD1 siRNA *versus* cells transfected with control siRNA.

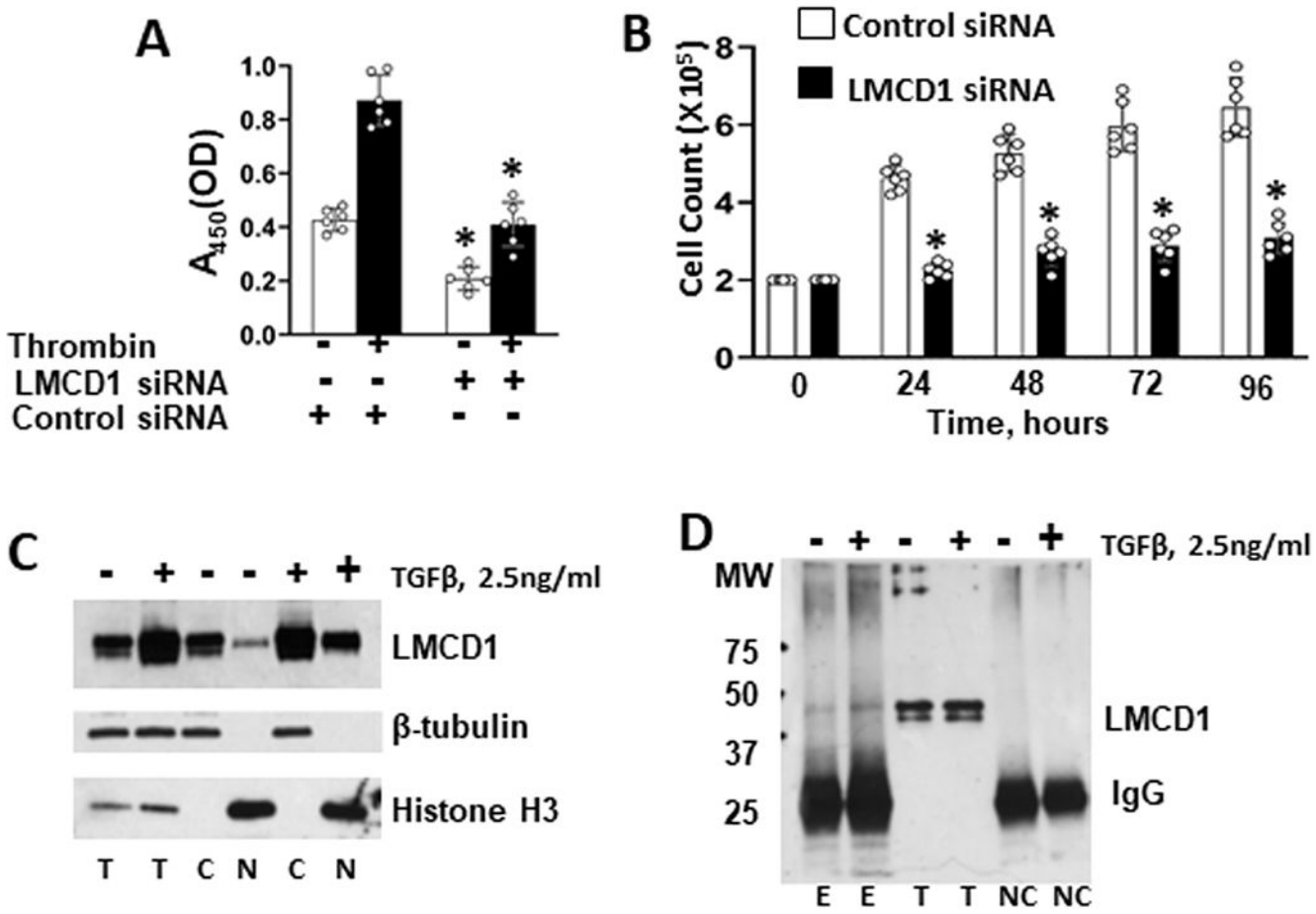

Figure 5.

A and B, effects of LMCD1 on cell proliferation. A, depletion of LMCD1 by siRNA reduces basal and thrombin-induced proliferation of SSc lung fibroblasts. **B**, LMCD1 siRNA inhibits thrombin-induced proliferation of SSc lung fibroblasts in a time-dependent manner. Data are presented as mean values ± SD of three independent experiments. The *asterisk* represents statistically significant differences ($p<0.001$) between cells transfected with LMCD1 siRNA *versus* cells transfected with control siRNA. **C**, **localization patterns of LMCD1 in SSc lung fibroblasts**. Cytoplasmic (C) and nuclear (N) fractions were isolated from cells cultured with or without TGFβ and immunoblotted with LMCD1 antibody. Total cell lysate (T) was loaded as a control. Tubulin and Histone-H3 antibodies were used to confirm purity of cytoplasmic and nuclear fraction. Representative immunoblots of three independent experiments are presented. **D, co-immunoprecipitation of LMCD1 and SRF in SSc lung fibroblasts**. Cells were cultured with or without TGFβ, immunoprecipitated (IP) with SRF antibody, and immunoblotted with LMCD1 antibody. E stands for eluted interactive complexes. Total cell lysate (T) was used as a positive control. Cell lysate incubated with Sepharose beads without IP antibody was used as a negative control (NC). The experiments were performed three times and representative immunoblots are presented.

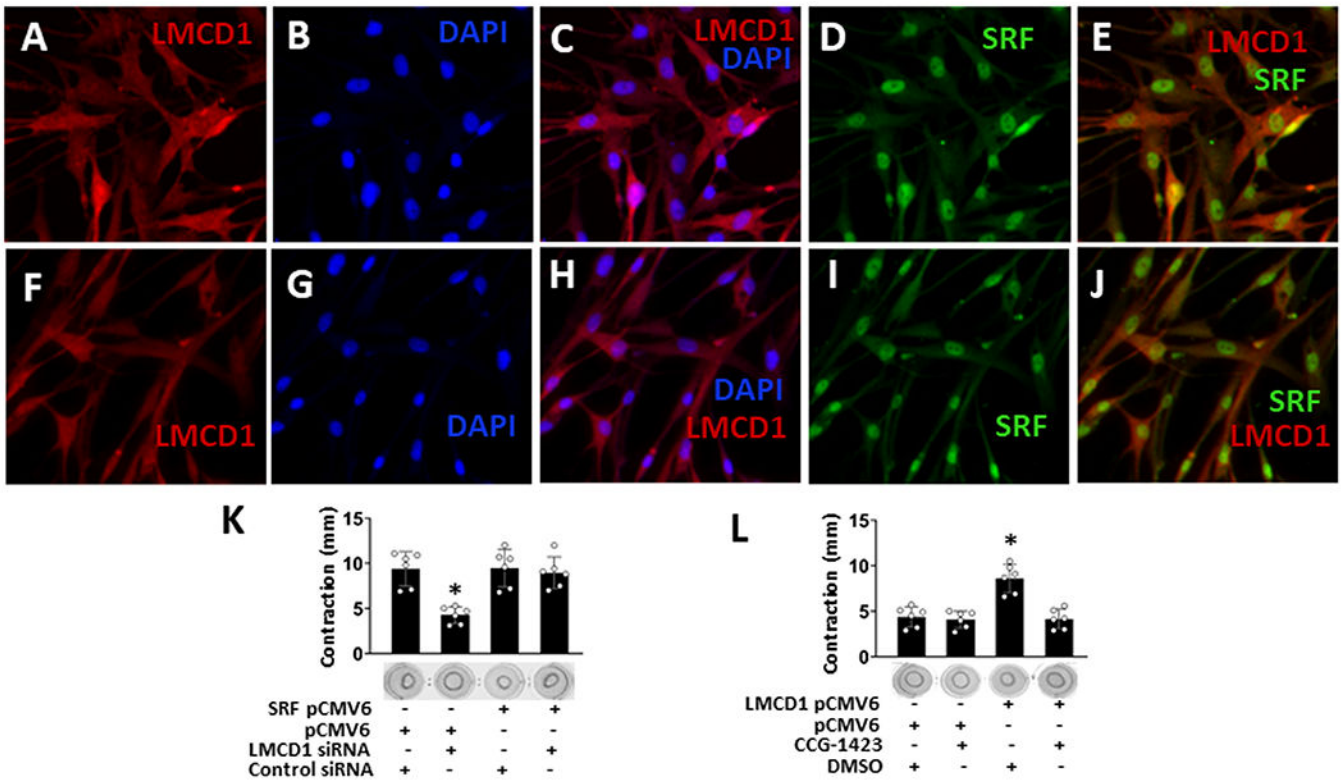

Figure 6.

A – J, co-localization of LMCD1 and SRF in scleroderma lung fibroblasts. Cells were incubated for 24 hours with 2.5 ng/ml TGFβ (**A - E**) or with vehicle (**F – J**) and stained with LMCD1 and SRF antibodies as detailed in the Methods. Representative images of three independent experiments are presented. **K, SRF restores contractile activity of scleroderma lung fibroblasts**. Cells were co-transfected with LMCD1 siRNA and recombinant SRF in pCMV6 and subjected to collagen gel contraction assay as detailed in Methods. Scrambled siRNA and empty vector were used as controls. **L, effect of SRF inhibitor on LMCD1-induced contractile activity.** Normal lung fibroblasts were transfected with recombinant LMCD1 in pCMV6 and cultured in collagen gels with or without 300 nM CCG-1423 for 48 hours. Empty pCMV6 and DMSO (CCG-1423 vehicle) were used as controls. Data in K and L are the mean and SD from three independent experiments each performed in duplicate. The *asterisk* represents statistically significant differences ($p<0.01$) as compared to controls.